VIA MEDICA

ORIGINAL ARTICLE

Folia Morphol.
Vol. 81, No. 2, pp. 280–293
DOI: 10.5603/FM.a2021.0044

ISSN 0015–5659
eISSN 1644–3284
journals.viamedica.pl

N-acetylcysteine protects against cuprizone--induced demyelination: histological and immunohistochemical study

S.H. El Sharouny[1], M.H. Shaaban[1], R.M. Elsayed[2], A.W. Tahef[2], M.K. Abd ElWahed[2]

[1]*Department of Anatomy and Embryology, Faculty of Medicine, Cairo University, Cairo, Egypt*
[2]*Department of Anatomy and Embryology, Faculty of Medicine, Fayoum University, Egypt*

[Received: 8 March 2021; Accepted: 9 April 2021; Early publication date: 29 April 2021]

Background: *Myelination is a sequential process that is tightly controlled by a number of intrinsic and extrinsic factors. Any central nervous system disease in which the neuronal myelin sheath is damaged is referred to as demyelinating disease. The present work was designed to study the histopathological, ultrastructural and immunohistochemical changes in rat brain, mainly corpus callosum (CC), following oral administration of cuprizone (CPZ), and the role of N-acetylcysteine (NAC) in reducing these changes.*

Materials and methods: *Demyelination was induced by CPZ administration for short (4 weeks) and long (8 weeks) periods. NAC was given concomitantly and sequentially for similar periods. Spontaneous recovery after cessation of CPZ followed by no medication was also investigated. At the end of each experimental period, both cerebral hemispheres were extracted and prepared for light and electron microscopic examination and immuno-histochemical study.*

Results: *The obtained results showed a direct proportion between the duration of CPZ administration and the severity of demyelination. The co-administration of CPZ and NAC, had a fair protective impact that was stronger than the sequential administration of the two drugs. Incomplete spontaneous remyelination was observed after cessation of CPZ, being more evident in short than in long period group, indicating that when CPZ administration is prolonged, remyelination is delayed.*

Conclusions: *In the light of the above results, it could be concluded that NAC has neuroprotective effects and has the potential to be a novel therapeutic approach for the treatment of demyelinating diseases such as multiple sclerosis; however, treatment should begin as soon as the disease manifests.* (Folia Morphol 2022; 81, 2: 280–293)

Key words: cuprizone, N-acetylcysteine, demyelination, remyelination, corpus callosum, rats

INTRODUCTION

Myelination is a process that is highly orchestrated by many intrinsic and extrinsic variables, step-by-step [19]. Many animal studies have shown that the neuronal activity along axons modulates its degree of myelination [3]. Although the mechanism of myelin formation is not yet fully understood; it is modelled as a staged process, from differentiation of oligodendro-

Address for correspondence: Ass. Prof. M.K. Abd ElWahed, Anatomy and Embryology, Faculty of Medicine, Fayoum University, Egypt, e-mail: mahakhaled007@yahoo.com

cyte (OL) progenitor cells to oligodendrocytes (OLs), followed by ensheathment of axons and ultimately maturation of the sheath [28].

Demyelinating disease is defined as any central nervous system (CNS) disease in which the neuronal myelin sheath is damaged [27]. Based on their pathogenesis, demyelinating CNS diseases can be categorised into: inflammatory diseases (e.g.: multiple sclerosis [MS] and acute-disseminated encephalomyelitis), viral infection, hypoxic-ischaemic types and demyelination caused by acquired metabolic disorders or focal compression of the brain [30]. Oligodendrocytes are vulnerable to oxidative stress-mediated damage, cytotoxicity, deprivation of the trophic factor and activation of apoptotic pathways [13]. Demyelination and inflammation are pathological features of MS and both are assumed to contribute to axon damage and consequently to cerebral atrophy that is prevalent in later stages of the disease [48]. MS demyelinating lesions are multifocal and spread in the brain affecting both white and grey matter. After demyelinating events, remyelination frequently occurs, but it is often incomplete. Consequently, understanding remyelination failure and designing strategies to restore myelin sheath is one of the challenges of MS science [22].

In MS pathogenesis, oxidative stress is a key factor that alleviates the migration of leukocytes, thereby leading to OLs damage and axonal injury. In the CNS of MS patients, reactive oxygen and nitrogen species are formed mainly by activated macrophages and microglia, the resident macrophage of the brain, and are responsible for demyelination and axon disruption. Various inflammatory and oxidative stress mediators such as cytokines and chemokines are secreted by activated microglia [6, 34].

Cuprizone (CPZ) is a copper-chelator of low molecular weight that affects the metabolism of cells and contributes to reversible demyelination in both grey and white matter [10]. Feeding with cuprizone results in the death of mature OLs, whereas other CNS cell types are not affected because oligodendroglia is more vulnerable to copper deficiency [59]. The toxic effect of CPZ on mature OLs results in the inhibition of the mitochondrial activity of the copper-dependent cytochrome oxidase and monoamine oxidase enzymes, resulting in mitochondrial dysfunction either through enlargement or clustering, this is followed by their apoptosis [2]. Oligodendrocytes death is thought to result from persistent mitochondrial stress brought on by both the toxic effect of the drug and the inherent immune response [57]. Microglia and reactive astrocytes populate in the demyelination areas and secrete pro-inflammatory cytokines (e.g.: tumour necrosis factor-α, interleukin-1β and interferon-γ) that govern the demyelination process [56].

N-acetylcysteine (NAC) is an effective free radicals scavenger of reactive oxygen species (ROS) but its key function as a therapeutic antioxidant stems from its role as a cysteine and glutathione synthesis precursor [12, 14]. Previous studies provide evidence for the therapeutic potential of NAC in multiple psychiatric and neurological disorders and claimed that to its anti-oxidant, anti-inflammatory and anti-apoptosis effects [4, 6, 9, 16, 38, 46].

Recently, Zhou et al. 2020 [61] indicated that NAC boosts remyelination process via promoting OL survival in oxidative stress-related conditions through the increase in glutathione levels and upregulation of haem oxygenase-1 (HO-1), a cytoprotective enzyme, that play a fundamental role in OLs protection.

The aim of the this work is to investigate the possible therapeutic role of NAC in CPZ-induced demyelination in the brain, particularly corpus callosum, of male albino rat and to elucidate the possible spontaneous recovery (remyelination) after cessation of cuprizone.

MATERIALS AND METHODS

Material

Chemicals. Cuprizone (bis-cyclohexanone-oxaldihydrazone) was supplied by Sigma-Aldrich Company in the form of powder, which was dissolved in distilled water and given orally by gastric gavage tube to the rats in a dose of 2 g/kg of body weight (bw) [39].

N-acetylcysteine was supplied by Sedico Company as effervescent instant granules 600 mg/mL, which were dissolved in distilled water and given orally by gastric gavage tube in a dose of 50 mg/kg bw [11]. The gastric gavage tube was left in position for 20 s to prevent regurgitation and ensure administration of the calculated doses.

Animals. Seventy adult male albino rats of Sprague Dawley strain, 4-months of age and weighing 150–250 g were used in the current study. They were obtained from the animal house, Faculty of Medicine, Cairo University and housed in metal cages, 5 rats/cage under standard laboratory and environmental conditions. The rats were used according to ethics of Animal Care and Use Committee (ACUC) of Cairo University.

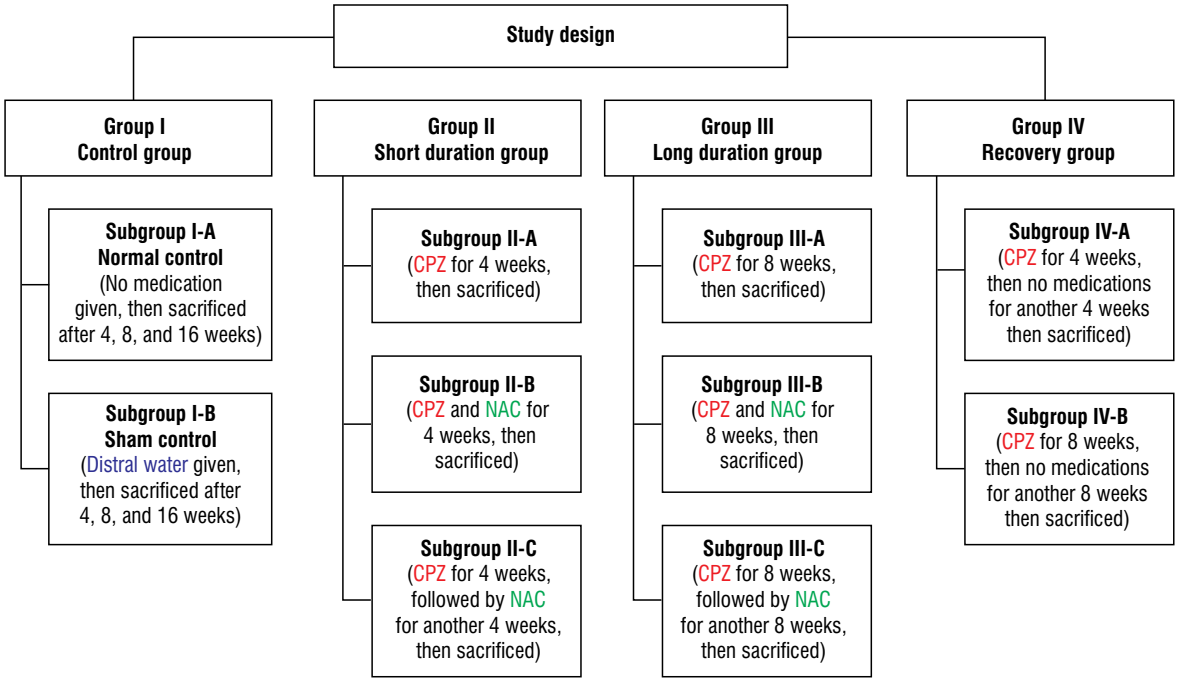

Figure 1. Flowchart of study design; CPZ — cuprizone; NAC — N-acetylcysteine.

Experimental design. Rats were divided into four groups:

- group I (Control group): comprised 30 rats and subdivided into two subgroups:
  - subgroup I-A (Normal control group): comprised 15 rats, they received no medications. Five rats were sacrificed after 4, 8 and 16 weeks respectively;
  - subgroup I-B (Sham control group): comprised 15 rats, they were given distilled water orally; daily for 4, 8 and 16 weeks respectively;
- group II (CPZ treated group, short duration): comprised 15 rats and divided into three subgroups as follows:
  - subgroup II-A: each rat received the calculated dose of CPZ orally; daily for 4 successive weeks;
  - subgroup II-B: each rat received the calculated doses of CPZ concomitant with NAC orally; daily for 4 successive weeks;
  - subgroup II-C: each rat received the calculated dose of CPZ daily orally for 4 successive weeks followed by the calculated dose of NAC orally; daily for another 4 successive weeks;
- group III (CPZ treated group, long duration): comprised 15 rats and subdivided into three subgroups; 5 rats each as follows:
  - subgroup III-A: each rat received the calculated dose of CPZ for 8 weeks;
  - subgroup III-B: each rat received the calculated doses of CPZ concomitant with NAC orally; daily for 8 successive weeks;
  - subgroup III-C: each rat received the calculated doses of CPZ followed by NAC orally; daily for 8 successive weeks;
- group IV (CPZ recovery group): comprised 10 rats and subdivided into two subgroups; 5 rats each:
  - subgroup IV-A: each rat received the calculated dose of CPZ daily orally for 4 successive weeks; then no medication received for another 4 successive weeks;
  - subgroup IV-B: each rat received the calculated dose of CPZ daily orally for 8 successive weeks; then no medication received for another 8 successive weeks (Fig. 1).

Methods

At the end of the experimental period, the rats were sacrificed after anaesthetisation with 50 mL/kg subcutaneous injection of thiopental sodium and the brains were extracted and rinsed under distilled water to remove any surface blood, followed by immersion in ice-cold normal saline for 5 min then placed on cold metal plate, finally two cerebral hemispheres were sectioned along the sagittal suture and prepared for the following studies.

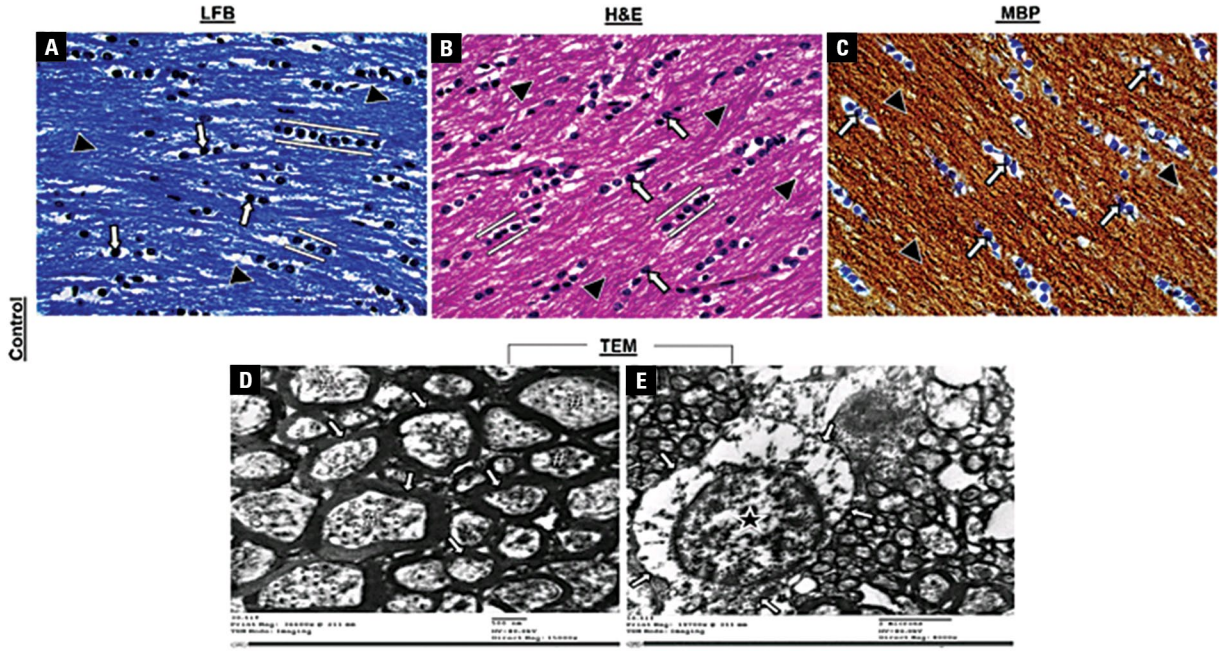

Figure 2. Myelinated nerve fibres of corpus callosum. Light microscopic examination of myelination in control groups; **A, B.** Densely packed, myelinated and parallel arranged fibres **(▲)**. The oligodendrocytes nuclei (arrows) appear well defined, rounded, darkly stained and arranged in longitudinal rows parallel (bracketed by lines) to the nerve fibres that they myelinate; **C.** Strong positive myelin basic protein reaction of myelin fibres **(▲)** and oligodendrocytes nuclei (arrows). Electron microscopic examination; **D.** Variable sized densely packed axons (#), surrounded by thick dense myelin sheath (arrows) with electron lucent intact cytoplasm; **E.** Normal oligodendrocyte with oval dark nucleus (★), regular nuclear envelope, clumped chromatin and surrounded by electron lucent cytoplasm (arrows); A. Luxol fast blue stain (LFB) ×400; B. Haematoxylin and eosin stain (H&E) ×400; C. Myelin basic protein (MBP) ×400; D. Electron microscopic examination (TEM) ×15000; E. TEM ×8000.

Light microscopic examination. The extracted brains were immersed in formalin 10%, for 2 days. Then washed under running tap water, and then embedded in paraffin. Sagittal sections of 7 microns thickness were made and stained with:

— luxol fast blue stain (LFB): to visualise the myelin in nerve sheath. Myelin stained blue while the nuclei and Nissl substance stained violet or red [26];
— haematoxylin and eosin stain (H&E): for standard histological examination [29].

Immuno-histochemical study [45]. Myelin basic protein antibody (MBP-antibody) (Thermo Fischer, Labvision, USA): is an unconjugated rabbit polyclonal antibody. A positive myelin fibres reaction is visible as a brown precipitate under the microscope, and the nuclei appear light blue.

Electron microscopic examination (TEM). Freshly prepared sections from brain samples of each group were fixed in 4% glutaraldehyde. Then processed and examined to detect ultrastructure changes [23].

RESULTS

Myelinated nerve fibres of corpus callosum (CC). Light microscopic examination of myelination in control groups revealed densely packed, myelinated and parallel arranged fibres. The OLs nuclei appeared well defined, rounded, darkly stained and arranged in longitudinal rows parallel to the nerve fibres that they myelinate (Fig. 2A, B). The nerve fibres and OLs nuclei showed strong positive myelin basic protein reaction (Fig. 2C). TEM showed variable sized densely packed axons. Axons were seen surrounded by thick electron dense myelin sheath and electron lucent intact cytoplasm (Fig. 2D). The OL appeared ovoid with dark nucleus surrounded by regular nuclear envelope and contains clumped chromatin material beneath the nuclear envelope and throughout the nucleoplasm. It is seen surrounded by electron lucent cytoplasm (Fig. 2E).

Concomitant administration of NAC protected from CPZ-induced demyelination more efficiently than the consecutive treatment by the two drugs. Light microscopic examination of demyelination in **CPZ-treated group for 4 weeks** showed multiple areas of unpacked partially demyelinated nerve fibres with axonal disruption and splitting, partial loss of OLs nuclei, most of them appeared dispersed and showed faint staining and karyorrhexis, others appeared cir-

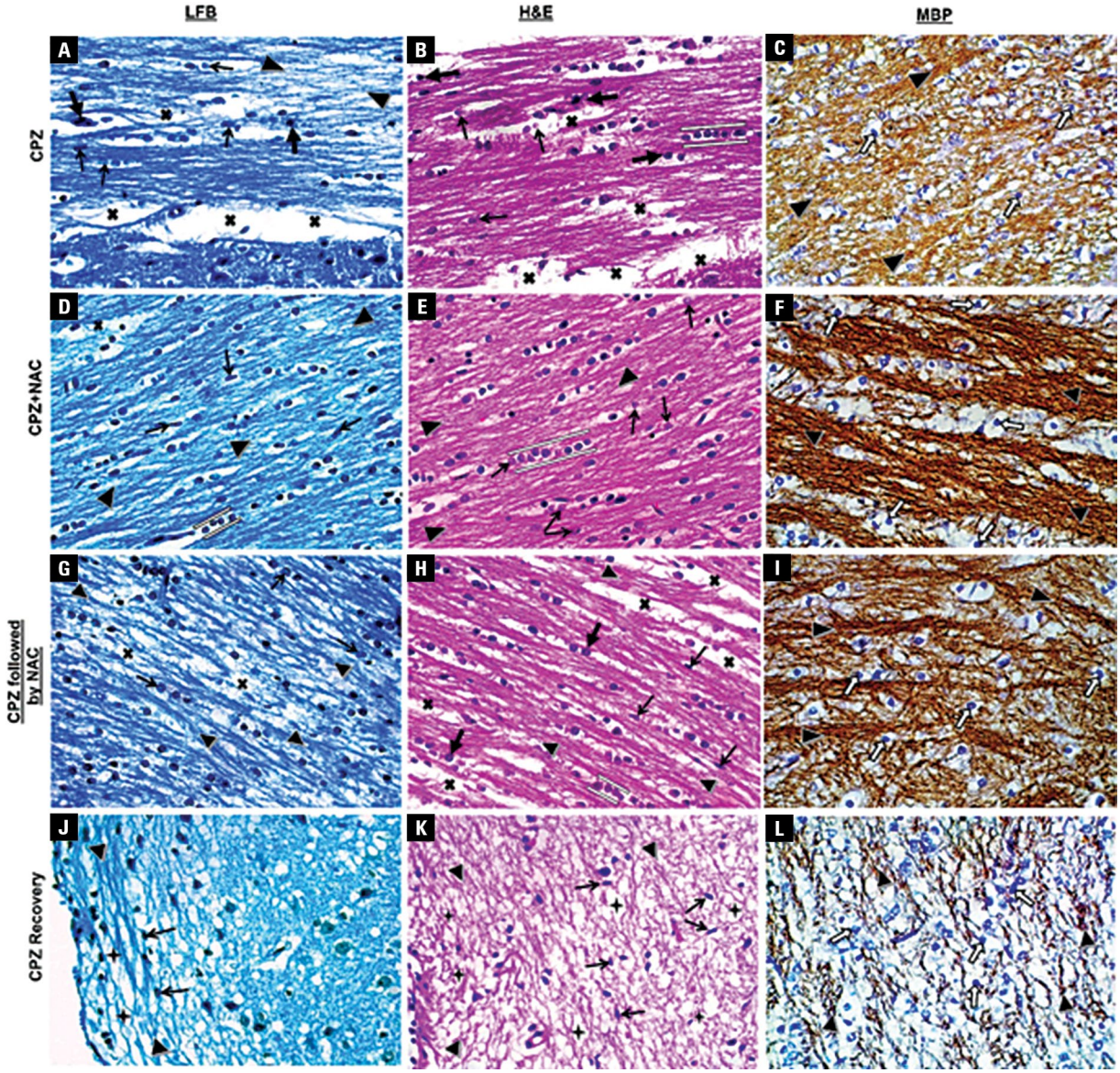

Figure 3. Concomitant administration of N-acetylcysteine (NAC) protects from cuprizone (CPZ)-induced demyelination more efficiently than the consecutive treatment by the two drugs. Light microscopic examination of demyelination in CPZ-treated group for 4 weeks; **A, B.** Multiple areas of unpacked partially demyelinated nerve fibres (▲) with axonal disruption and splitting (X), partial loss of oligodendrocytes nuclei, most of them appear dispersed and showing faint staining and karyorrhexis (thin arrows), others are circumscribed and darkly stained (thick arrows), few nuclei are seen oriented parallel to the nerve fibres (bracketed by lines); **C.** Moderate positive myelin basic protein reaction of myelin fibres **(▲)** and oligodendrocytes nuclei (arrows). CPZ and NAC treated group; **D.** Well-arranged, packed demyelinated nerve fibres **(▲)** with focal axonal disruption and fragmentation (X); **E.** Preserved disorganised oligodendrocytes nuclei with some of them arranged in linear rows (bracketed by lines). Most of them appear rounded and darkly stained with few flattened small sized nuclei showing faint staining and karyorrhexis (arrows); **F.** Strong myelin basic protein positive reaction of myelin fibres **(▲)** and positive oligodendrocytes nuclei (arrows) reaction. CPZ followed by NAC-treated group; **G, H.** Demyelinated unpacked nerve fibres (▲) with focal axonal splitting (X) and dispersed faintly stained oligodendrocyte nuclei (arrows). Oligodendrocyte nuclei are seen parallel to the nerve fibres (bracketed by lines). Most of them appear round and circumscribed with faint staining (thick arrows) and few appear flattened (thin arrows); **I.** Strong positive myelin basic protein reaction of myelin fibres (▲) and oligodendrocytes nuclei (arrows). Weak spontaneous remyelination is detected in the short duration (CPZ 4 weeks) recovery group after 4 weeks of CPZ cessation; **J, K.** Disorganised, fragmented, demyelinated nerve fibres **(▲)** with wide areas of vacuolation **(★)**. Notable loss of oligodendrocytes nuclei with the remaining ones appear dispersed, flattened and of small size with faint staining (arrows); **L.** Weak myelin basic protein positive reaction of myelin fibres (▲) and moderate oligodendrocytes nuclei (arrows). A, D, G, J. Luxol fast blue stain (LFB) ×400; B, E, H, K. Haematoxylin and eosin stain (H&E) ×400; C, F, I, L. Myelin basic protein (MBP) ×400.

cumscribed and darkly stained. Few nuclei are seen oriented parallel to the nerve fibres (Fig. 3A, B). The nerve fibres and OLs nuclei showed moderate positive myelin basic protein reaction (Fig. 3C). CC

nerve fibres of **CPZ and NAC treated group** displayed that most of the nerve fibres exhibited fair myelination and appeared well arranged and packed. Few specimens showed focal axonal disruption and fragmentation. The OLs nuclei appeared preserved but disorganised. Some of them are seen oriented in linear rows parallel to the nerve fibres. The nuclei appeared rounded with darkly stained. Few nuclei appeared flattened and small in size with faint staining and karyorrhexis (Fig. 3D, E). The nerve fibres showed strong positive myelin basic protein reaction associated with positive OLs nuclei reaction (Fig. 3F). **CPZ followed by NAC-treated group** revealed demyelinated and unpacked nerve fibres with localized areas of axonal disruption and splitting. The OLs nuclei were preserved but dispersed. Some of them were seen oriented parallel to the nerve fibres. Most of the nuclei appeared rounded faintly stained (Fig. 3G, H). The nerve fibres showed moderate positive myelin basic protein reaction and positive OLs nuclei reaction (Fig. 3I). **Weak spontaneous remyelination was detected in the short duration (CPZ4Ws) recovery group after 4 weeks of CPZ cessation.** The CC nerve fibres of this recovery group appeared fragmented, demyelinated and disorganized with large cytoplasmic vacuoles being more evident near the periventricular region. Oligodendrocytes nuclei appeared of small size, rounded, darkly stained and dispersed, while others appeared flattened (Fig. 3J, K). The nerve fibres displayed weak positive myelin basic protein reaction and moderate positive OLs nuclei reaction (Fig. 3L).

Electron microscopic examination of the **CPZ-treated group for 4 weeks** revealed that the nerve fibres were unpacked with narrow gapping in between, multiple thin myelinated and scanty unmyelinated axons were seen. Few thick myelinated axons were also seen. Most of the myelin sheaths appeared redundant or irregular and displayed focal areas of lamellar splitting. Some axons showed axonal cytoplasmic degeneration, others showed inclusion bodies in their cytoplasm (Fig. 4A). The OLs in this group appeared ovoid containing dark nucleus with regular nuclear envelope and clumped chromatin both beneath the nuclear envelope and throughout the nucleoplasm. They were seen surrounded by multiple variable sized thin and thick myelinated axons with degenerated cytoplasm (Fig. 4B). The CC nerve fibres of **CPZ and NAC-treated group** were predominantly thin myelinated with few well myelinated ones. Some of their myelin sheaths appeared redundant with splitting and showed variable degrees of axonal cytoplasmic degeneration and inclusion bodies (Fig. 4C). The OLs nuclei were ovoid and dark with regular nuclear envelope and surrounded by rarified cytoplasm. They were seen in close relation to the surrounding axons (Fig. 4D). The **CPZ followed by the NAC-treated group** displayed unpacked nerve fibres with narrow gaps in between. A lot of thin myelinated and unmyelinated axons were seen. The myelin sheaths appeared redundant with focal lamellar splitting. Variable degrees of cytoplasmic degeneration were seen (Fig. 4E). The OLs nuclei appeared ovoid and dark with regular nuclear envelope and clumped chromatin. The surrounding cytoplasm showed connection to multiple variable sized thin myelinated axons (Fig. 4F). **The CPZ-recovery group (4 weeks after CPZ cessation)** displayed unpacked axons with wide areas of gapping in between. The demyelination patches showed predominantly thin myelinated axons, few unmyelinated axons with ratified axonal cytoplasm. Myelin sheaths appeared irregular, split and abnormally folded. Rarified axonal cytoplasm with absence of inclusion bodies was observed (Fig. 4G). The OLs nuclei appeared ovoid and dark with regular nuclear envelope and clumped chromatin. The surrounding cytoplasm appeared electron lucent with multiple vacuoles and few abnormal folded myelin sheaths with no evidence of axonal connection (Fig. 4H).

CPZ supplementation for long duration (8 weeks) produced massive demyelination and lessened the protective effects of NAC. Light microscopic examination of demyelination in **CPZ-treated group for 8 weeks** revealed marked demyelination, fragmentation and complete disorganisation of CC nerve fibres. All OLs nuclei appeared disorganised and of small size, irregular shaped with faint staining and variable degrees of karyorrhexis and karyolysis (Fig. 5A, B). The nerve fibres showed negative myelin basic protein reaction with poor OLs nuclei reaction (Fig. 5C). **CPZ and NAC-treated group** showed that the CC nerve fibres appeared partially demyelinated and unpacked, with scanty areas of splitting in the myelin sheath and vacuolated cytoplasm. The OLs nuclei appeared preserved and arranged in linear rows between the unpacked nerve fibres. They appeared rounded, darkly stained apart from scanty nuclei which showed faint staining and others appeared flattened (Fig. 5D, E). The nerve fibres

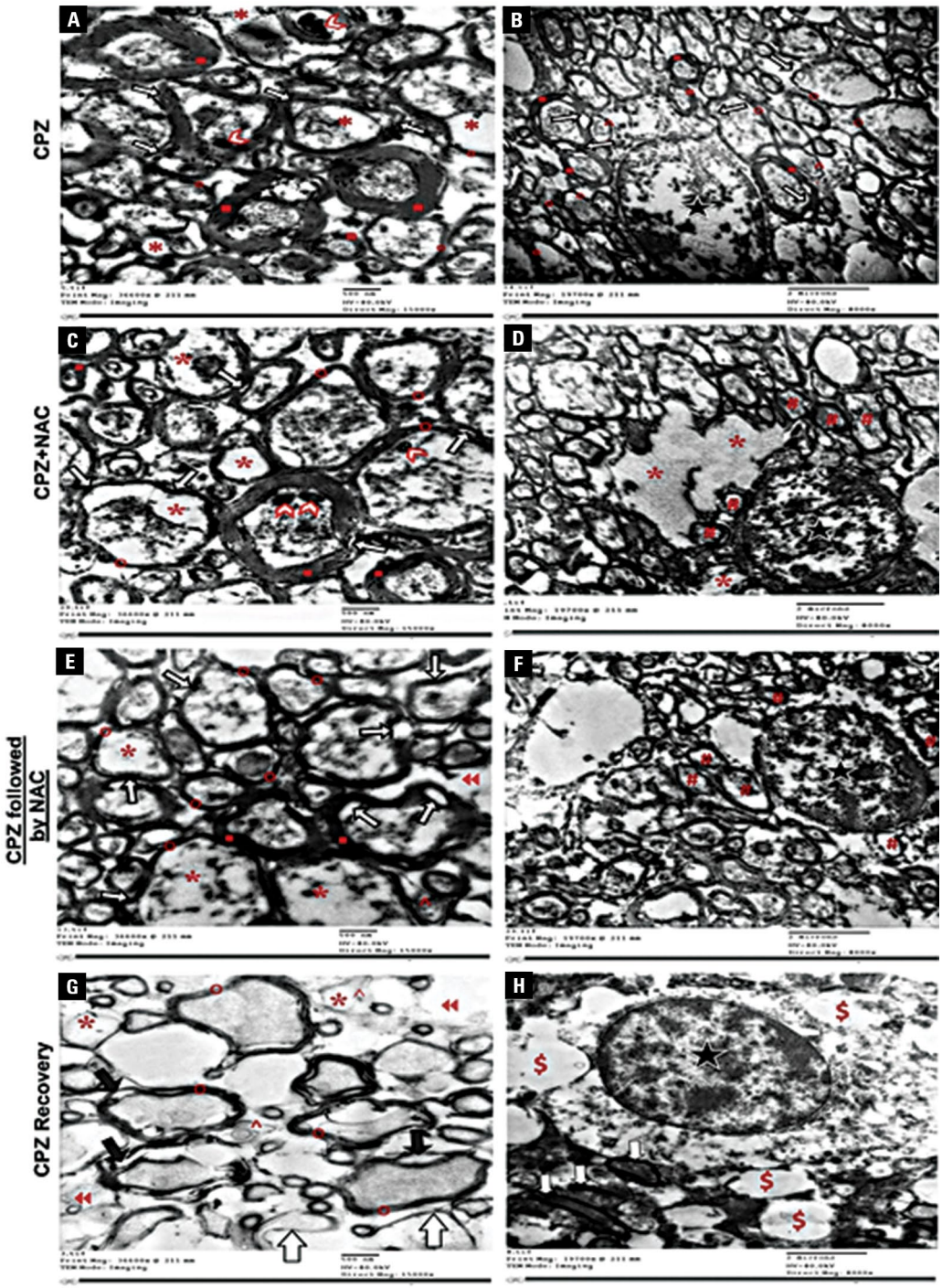

Figure 4. Electron microscopic examination of short duration cuprizone (CPZ)-treated group (4 weeks); **A.** Narrow gapping between unpacked thin myelinated (o) and thick myelinated (▪) axons exhibiting redundant sheath (arrows) with some of them showing partial axonal degeneration (*) and inclusion bodies (⪡); **B.** Oligodendrocyte (★) containing dark nucleus surrounded by few thick myelinated axons (▪) with redundant myelin sheath and focal areas of splitting (arrows), unmyelinated (^) and multiple irregular thin myelinated (o) axons. CPZ and N-acetylcysteine (NAC)-treated group; **C.** Multiple thick myelinated **(▪)** and thin myelinated **(o)** axons with some of them exhibiting split, redundant sheath (arrows) as well as degenerated axonal cytoplasm (*) and inclusion bodies (⪡); **D.** Ovoid, dark nucleus (★) surrounded by rarified cytoplasm (*) and is adherent to the nearby axons (#). CPZ followed by the NAC-treated group; **E.** Unpacked axons with narrow gapping in between (◀◀). Multiple thin myelinated (o) and few unmyelinated (^) axons are seen, few axons exhibit redundant split myelin sheath (arrows) and axonal cytoplasmic degeneration (*); **F.** Ovoid, dark nucleus **(★)** with the surrounded cytoplasm displayed connection to multiple variable sized thin myelinated axons (#). The short duration CPZ-recovery group; **G.** Multiple thin myelinated (o) and few unmyelinated (^) axons with rarified axonal cytoplasm (*) and wide gaps in between (◀◀). The myelin sheaths are irregular with notable splitting (black arrows), abnormal folded myelin sheaths are seen (white arrows); **H.** Ovoid, dark nucleus (★), surrounded by electron lucent cytoplasm showing multiple vacuoles ($) and abnormal folded myelin sheaths (white arrows) with no evidence of axonal connection. A, C, E, G. Electron microscopic examination (TEM) ×15000; B, D, F, H. TEM ×8000.

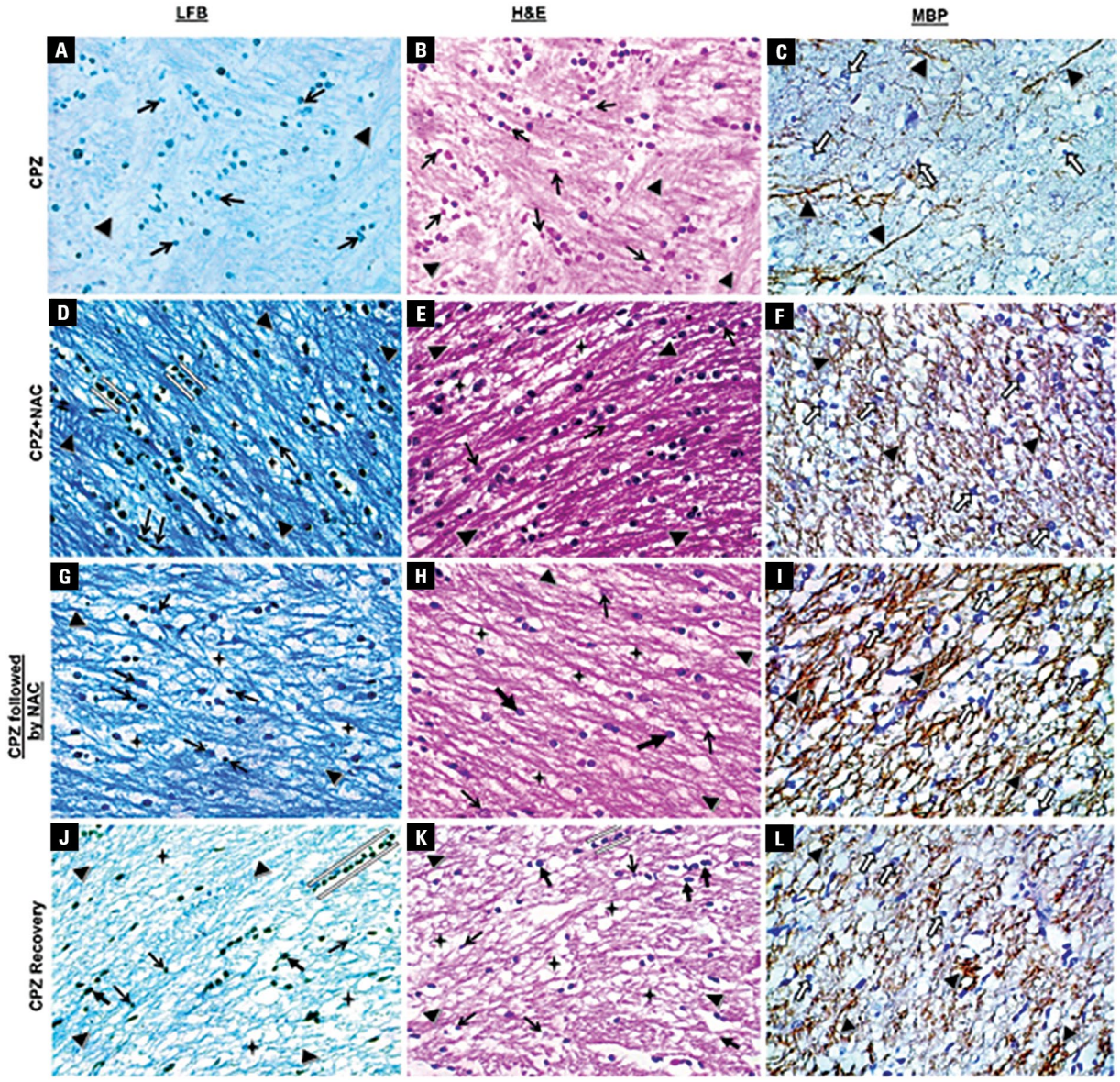

Figure 5. Cuprizone (CPZ) supplementation for long duration produces massive demyelination and lessens the protective effects of N-acetylcysteine (NAC). Light microscopic examination of demyelination in long duration CPZ-treated group (8 weeks); **A, B.** Markedly demyelinated, disorganised and fragmented nerve fibres (▲). Loss of oligodendrocytes nuclei with the remaining ones appear disorganised, of small size with variable degrees of karyorrhexis and karyolysis (arrows); **C.** Negative myelin basic protein reaction of myelin fibres (▲) and oligodendrocytes nuclei (arrows). CPZ and NAC treated group; **D, E.** Partially demyelinated unpacked nerve fibres **(▲)** with scanty areas of vacuolation (★). Most oligodendrocyte nuclei appear rounded, darkly stained with few displaying faint staining (arrows) and seen parallel to the nerve fibres (bracketed by lines) with few nuclei appear flattened (arrows); **F.** Weak positive myelin basic protein reaction of myelin fibres (▲) and moderate positive oligodendrocytes nuclei (arrows). CPZ followed by NAC-treated group; **G, H.** Unpacked diffusely demyelinated nerve fibres (▲) with axonal splitting and vacuolation (★). Dispersed oligodendrocyte nuclei, which appear rounded, circumscribed with faint staining (thick arrows) and few appear of small size and exhibit karyorrhexis and karyolysis (thin arrows); **I.** Positive reaction of oligodendrocytes nuclei (arrows) with weak positive myelin fibres (▲). Poor spontaneous remyelination is detected in the long duration (CPZ 8 weeks) recovery group after 8 weeks of CPZ cessation; **J, K.** Markedly disorganised demyelinated nerve fibres (▲) with diffuse vacuolation (★). The oligodendrocyte nuclei appear dark (thick arrows) and parallel aligned to nerve fibres (bracketed by lines), while others appear of small size with faint staining (thin arrows); **L.** Weak positive myelin basic protein reaction of myelin fibres (▲) and oligodendrocytes nuclei (arrows). A, D, G, J. Luxol fast blue stain (LFB) ×400; B, E, H, K. Haematoxylin and eosin stain (H&E) ×400; C, F, I, L. Myelin basic protein (MBP) ×400.

showed weak positive myelin basic protein reaction with moderate positive OLs nuclei reaction (Fig. 5F). **CPZ followed by NAC-treated group** showed that the CC nerve fibres appear diffusely demyelinated, unpacked and disorganised with wide areas of axonal fragmentation, splitting and cytoplasmic vacuolation.

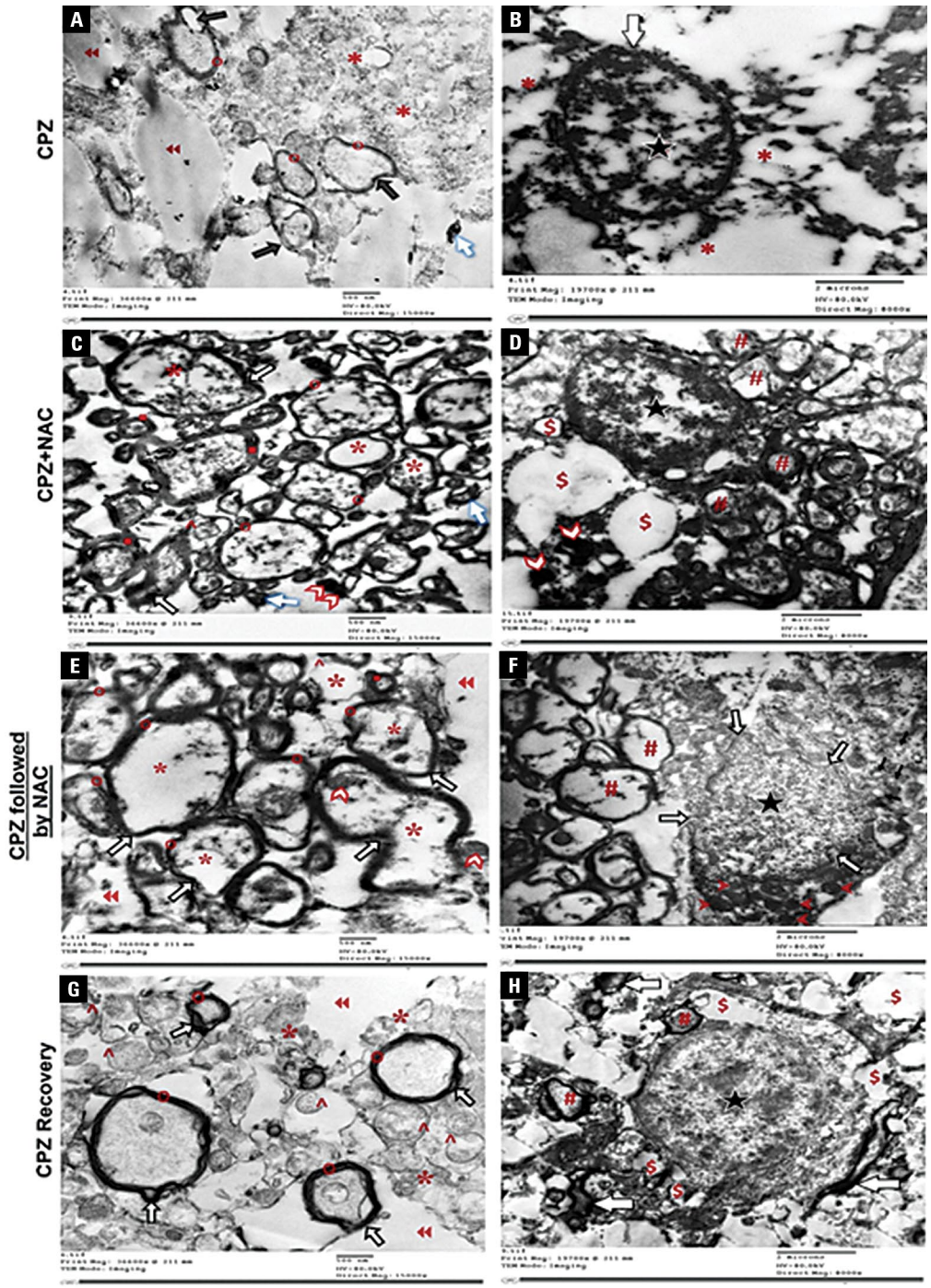

Figure 6. Electron microscopic examination cuprizone (CPZ)-treated group for 8 weeks; **A.** Scanty thin myelinated (o) axons with split redundant myelin sheath (arrows). Wide gaps of complete axonal loss (◀◀) containing extensive remnants of fragmented degenerated axons (*) and folded collapsed myelin sheath (white arrows); **B.** Oval heterochromatic oligodendrocyte nucleus (★) with focal nuclear envelop indentation (white arrow) and surrounded by completely degenerated rarified cytoplasm (*). CPZ and N-acetylcysteine (NAC) treated group; **C.** Irregularly arranged unpacked multiple thin myelinated (o), few myelinated (▪) and unmyelinated (^) axons. Most axons showing redundant sheath (arrows) inclusion bodies (⪡) and compact myelin sheath (white arrows); **D.** Ovoid, dark nucleus (★) with large cytoplasmic vacuoles ($) and inclusion bodies (⪡) and connection to demyelinated axons (#). CPZ followed by the NAC-treated group; **E.** Wide areas of irregularly arranged axons with gaps in between (◀◀). Multiple thin myelinated (o), few unmyelinated (^) (▪) axons almost all of them have irregular deformed myelin sheaths with diffuse axonal cytoplasmic degeneration (*) and scanty inclusion bodies (⪡); **F.** An ovoid nucleus (★) with irregular nuclear envelope (white arrows) and electron dense cytoplasm contain multiple mitochondria (◂), secretory granules (black arrows), and is seen connected to multiple thin myelinated axons (#). The CPZ-recovery group; **G.** Wide gapping (◀◀) between multiple thin myelinated (o) axons with irregular-split and tight-deformed myelin sheaths (arrows) and rarefied axonal cytoplasm (*). Multiple fragmented unmyelinated axons (^) are seen; **H.** Rounded, dark nucleus (★) surrounded by vacuolated cytoplasm ($) with multiple abnormal folded myelin sheaths (white arrows) and connected to few axons (#). A, C, E, G. Electron microscopic examination (TEM) ×15000; B, D, F, H. TEM ×8000.

Few nerve fibres appeared well arranged. Partial loss of OLs nuclei, with the remaining ones appearing dispersed. Some of them appeared rounded and circumscribed, Others appeared of small size with poor staining and karyolysis (Fig. 5G, H). The nerve fibres displayed weak positive myelin basic protein reaction and positive OLs nuclei reaction (Fig. 5I).

Poor spontaneous remyelination was detected in the long duration (CPZ 8 weeks) recovery group after 8 weeks of CPZ cessation. The nerve fibres of the long duration recovery group appeared markedly disorganised and demyelinated with diffuse poor staining and marked cytoplasmic vacuolation. Few OLs nuclei were seen parallel to the nerve fibres, most of them were dispersed and small sized with partial loss of their population. The nuclei exhibited dark and faint staining (Fig. 5J, K). The nerve fibres and OLs nuclei showed weak positive myelin basic protein reaction (Fig. 5L).

Electron microscopic examination of the **CPZ-treated group for 8 weeks** revealed massive axonal degeneration. The remaining axons were thin myelinated with split myelin sheath and wide gaps in between, these gaps contain remnants of fragmented degenerated axons and fragmented collapsed myelin sheaths (Fig. 6A). The OLs displayed oval heterochromatic nuclei with localised nuclear envelope indentation. Most OLs exhibited completely degenerated rarified cytoplasm (Fig. 6B). **CPZ and NAC-treated group** showed disorganised nerve fibres with narrow gaps in between. Multiple thin myelinated and unmyelinated axons were detected. Few specimens demonstrated multiple compact folded myelin sheath fragments and inclusion bodies (Fig. 6C). The OLs nuclei appeared ovoid and dark with regular nuclear envelope and clumped chromatin. The surrounding cytoplasm showed large vacuoles and inclusion bodies with close connection to the demyelinated axons (Fig. 6D). **CPZ followed by NAC-treated group** showed a lot of unpacked thin myelinated and demyelinated axons. Scanty myelinated small sized axons with irregular deformed myelin sheaths were seen. Axons displayed cytoplasmic rarefaction with scanty inclusion bodies (Fig. 6E). The OLs nuclei appeared ovoid and dark with irregular nuclear envelope and diffuse chromatin clumps. The surrounding cytoplasm appeared electron dense with abundant mitochondria and secretory granules. It was seen connected to multiple thin myelinated axons (Fig. 6F). **The CPZ-recovery group (after 8 weeks of CPZ cessation)** showed unpacked axons with wide gaps in between. The demyelination patches showed predominantly multiple fragmented unmyelinated axons and scanty thin myelinated axons. Some myelin sheaths appeared irregular and split. Almost all axons showed cytoplasmic rarefaction (Fig. 6G). Oligodendrocytes nuclei appeared rounded, dark and surrounded by electron dense vacuolated cytoplasm that contains multiple abnormal folded myelin sheaths with evidence of connection to few axons (Fig. 6H).

DISCUSSION

The development of animal models of human diseases is critical. Over the past 60 years, studies of MS and other demyelinating CNS disorders have closely followed this approach [35].

In the current study, CPZ intoxication model was used to induce CNS demyelination. That was in accordance with MacArthur and Papanikolaou (2014) [31], who stated that marked nerve demyelination in animals is induced by oral administration of CPZ, likewise, Vega-Riquer et al. (2019) [55] indicated that CPZ targets many enzymes such as ceruloplasmin, which impairs the activity of the copper dependent cytochrome oxidase, decreases oxidative phosphorylation and causes degenerative OL changes. Eventually, this cascade of events results in demyelination. Male albino rats were used in the present research to study the various aspects of demyelination in the CC, which was similar to other study by Franco et al. (2008) [17]. Hibbits et al. (2009) [24] and Steelman et al. (2012) [48] have documented that female rats are more resistant to CPZ-induced toxic demyelination, which could be due to potential hormonal and genetic influences.

In line with the current study, Skripuletz et al. (2011) [43] focused on the demyelinating effects of CPZ in the CC, as it is an OL-rich structure and the degree of demyelination may easily be achieved.

Systemic intoxication by CPZ was produced by daily administration of the drug for 4 and 8 week's durations to induce CC nerve demyelination, this was in agreement with Oakden et al. (2017) [39]. On the other hand, Taraboletti et al. (2017) [49] used CPZ fed mice model for 2 and 6 weeks and demyelination was observed at the third week and maximum demyelination reached at the 5th or 6 weeks. Administration of CPZ in subgroup III-A produced severe pathological changes more than in subgroup II-A indicating the presence of direct proportion between the duration

of administration and the severity of nerve demyelination, this was compatible with Zendedel et al. (2013) [59] who reported that partial demyelination of CC nerve fibres occurred after 2 weeks of CPZ intoxication, and called this process as (acute demyelination); while complete demyelination occurred after 5 to 6 weeks. On the other hand, Acs and Komoly (2012) [1] documented the incidence of severe demyelination after 3 weeks of CPZ administration associated with massive macrophage infiltration and astrocytosis in the demyelinated areas.

In the current model of CPZ intoxication, The examined groups illustrated variable degrees of axonal degeneration, loss of OLs and gapping between nerve fibres; these were in accordance with Freeman et al. (2015) [18]; Van Munster et al. (2015) [52]; Grothe et al. (2016) [21] and Vargas and Tyor (2017) [54]. These changes were more pronounced in subgroup III-A. Ultra-structurally, subgroup III-A revealed thin myelinated axons with axonal degeneration, fragmentation, axonal loss, fragmented collapsed myelin sheaths and OLs nuclear changes. Subgroup II-A, on the other hand, displayed mainly thick myelinated nerve fibres with redundant myelin sheaths and broken focal areas of splitting. Zendedel et al. (2013) [59] declared that demyelinated axons are more susceptible to damage due to the absence of trophic support from myelin sheaths, which are vital for maintaining axonal integrity. Craner et al. (2004) [8] reported a hypothesis of demyelination-related axonal damage, which could be due to the demyelinated axons' increased energy requirements to perform action potential, which could make demyelinated axons more prone to destructive processes.

In addition, gapping between the demyelinated nerve fibres in subgroup III-A were more than subgroups II-A, which was in accordance to a study made by Mierzwa et al. (2015) [33] who explained that the abnormal gaps between nerve fibres could slow information-processing speed, which is a common deficit in MS patients. Similar observations were clarified by Tobin et al. (2011) [51] and Hibbits et al. (2012) [25], who stated that CPZ induces extreme microglial phagocytosis of damaged myelin, and most cases of axons damage do not regenerate again.

Glutathione is an antioxidant that naturally exists in neurons that protects against oxidative harm. In the brain and the periphery of MS patients, glutathione levels have been found to be depleted [50]. Monti et al. (2020) [37] stated that, due to restricted antioxidants such as glutathione, the brain of MS patients was susceptible to high oxidative stress. Cacciatore et al. (2012) [5] and Wu and Batist (2013) [58] demonstrated that direct administration of glutathione is difficult due to its poor absorption and stability, which limits its bioavailability. Therefore, in a trial to raise endogenous glutathione levels, NAC is used in current research. This was consistent with Skvarc et al. (2017) [44] who reported that NAC was a glutathione precursor with potent antioxidant, pro-neurogenesis and anti-inflammatory properties. likewise, Zhou et al. (2020) [61] clarified that NAC promoted murine OL survival in oxidative stress-related conditions through the elevation of glutathione levels and upregulation of HO-1, a cytoprotective enzyme, played a principle role in OL protection and consequently boosted remyelination.

In the present study, the combined administration of NAC with CPZ in subgroups II-B and III-B reduced CC demyelination changes as compared to subgroups II-C and III-C. NAC led to retrieving almost the normal histological architecture of corpus callosum nerve fibres and OLs population, which were pronounced in subgroup II-B more than subgroup III-B demonstrating a duration dependency. This was in line with Stanislaus et al. (2005) [47] who reported that NAC treatment decreased inflammatory monocyte/macrophage cells in the CNS of rats with acute encephalomyelitis. Similarly, Saraswathy et al. (2014) [42] revealed that NAC at doses of 100 and 200 mg/kg could protect the brain tissue against phenytoin-induced brain damage. In vitro studies have indicated that NAC can promote the survival of neurons and OLs by preventing a decrease in the expression of their myelin-related genes, potentially facilitating remyelination. NAC can also attenuate OL degeneration caused by lipopolysaccharide in the developing rat brain [40]. In addition to Mohammed et al. (2019) [36] who demonstrated that supplementation with NAC reduced both histopathological abnormalities and biochemical findings induced by doxorubicin in cerebral cortex of albino rats and Fan et al. (2020) [15] who suggested that NAC therapy reduced neuronal damage caused by neuroinflammation and apoptosis, which was linked to decreased dendritic spine atrophy and synapse deficits in animal model of depression.

With regard to group IV, in the current thesis, consecutive administration of CPZ and NAC showed partial improvement in demyelination events less than that observed in group III with co-administration of both drugs. This was supported by Cilio and Ferriero

(2010)'s [7] previous work in neonates suffering from hypoxic injury after intrauterine infection. Monti et al. (2020) [37] used NAC for 2 months in MS patients. However, those patients have neurological symptoms for years and it might be necessary to expand the duration of administration of NAC for several months or even years in order to observe its maximum effectiveness in symptom control.

Cuprizone recovery group in the present work showed incomplete spontaneous remyelination of corpus callosum nerve fibres being more evident in subgroup IV-A than in subgroup IV-B. In a previous work of Manrique-Hoyos et al. (2012) [32] they demonstrated that following cessation of CPZ supplementation for 5 weeks, animals showed an initial recovery of locomotor performance with partial remyelination, a finding which was in line with the current study. Similarly, Zhen et al. (2017) [60] demonstrated that removal of CPZ from the diet of animals enhances remyelination of CC. Poor remyelination was evident in subgroup IV-B following withdrawal of CPZ. Vana et al. (2007) [53] and Zendedel et al. (2013) [59] reported that when CPZ administration was prolonged, remyelination was delayed, a process called (chronic demyelination) where the number of damaged axons is high. Goldschmidt et al. (2009) [20] and Vega-Riquer et al. (2019) [55] suggested that remyelination was a transient phenomenon and remyelinated shadow plaques might be affected by new bouts of demyelination, which ultimately leads to incomplete myelin sheath repair.

The current immuno-histochemical study showed a decreased myelin basic protein reaction in CC nerve fibres and OLs nuclei over time. The myelin basic protein reaction was improved in subgroups II-B and II-C more than subgroups III-B and III-C. In addition, there was minimal improvement in subgroup IV-A with no notable improvement in subgroup IV-B. Similar findings were recorded by Pohl et al. (2011) [41] who documented progressive reduction of immune-labelling for MBP over time in the cerebellar white matter, brainstem, midbrain and spinal cord white and grey matter. In addition to widespread progressive vacuolation (status spongiosus) in white matter that was present at the onset of clinical signs and increased in size and number over time.

CONCLUSIONS

In conclusion, administration of CPZ induced demyelination of CC nerve fibres with evidence of direct proportion between the duration of CPZ administration and the severity of demyelination. The co-administration of CPZ and NAC had a fair protective impact that was stronger than the sequential administration of the two drugs. On the basis of these observations, NAC has neuroprotective effects and has the potential to be a novel therapeutic approach for the treatment of demyelinating disease such as multiple sclerosis; however, treatment should begin as soon as the disease manifests.

Conflict of interest: None declared

REFERENCES

1. Acs P, Komoly S. Selective ultrastructural vulnerability in the cuprizone-induced experimental demyelination. Ideggyogy Sz. 2012; 65(7-8): 266–270, indexed in Pubmed: 23074847.
2. Acs P, Kipp M, Norkute A, et al. 17beta-estradiol and progesterone prevent cuprizone provoked demyelination of corpus callosum in male mice. Glia. 2009; 57(8): 807–814, doi: 10.1002/glia.20806, indexed in Pubmed: 19031445.
3. Auer F, Vagionitis S, Czopka T. Evidence for myelin sheath remodeling in the CNS revealed by in vivo imaging. Curr Biol. 2018; 28(4): 549–559.e3, doi: 10.1016/j.cub.2018.01.017, indexed in Pubmed: 29429620.
4. Bavarsad Shahripour R, Harrigan MR, Alexandrov AV. N-acetylcysteine (NAC) in neurological disorders: mechanisms of action and therapeutic opportunities. Brain Behav. 2014; 4(2): 108–122, doi: 10.1002/brb3.208, indexed in Pubmed: 24683506.
5. Cacciatore I, Baldassarre L, Fornasari E, et al. Recent advances in the treatment of neurodegenerative diseases based on GSH delivery systems. Oxid Med Cell Longev. 2012; 2012: 240146, doi: 10.1155/2012/240146, indexed in Pubmed: 22701755.
6. Cherry JD, Olschowka JA, O'Banion MK. Neuroinflammation and M2 microglia: the good, the bad, and the inflamed. J Neuroinflammation. 2014; 11: 98, doi: 10.1186/1742-2094-11-98, indexed in Pubmed: 24889886.
7. Cilio MR, Ferriero DM. Synergistic neuroprotective therapies with hypothermia. Semin Fetal Neonatal Med. 2010; 15(5): 293–298, doi: 10.1016/j.siny.2010.02.002, indexed in Pubmed: 20207600.
8. Craner MJ, Newcombe J, Black JA, et al. Molecular changes in neurons in multiple sclerosis: altered axonal expression of Nav1.2 and Nav1.6 sodium channels and Na+/Ca2+ exchanger. Proc Natl Acad Sci U S A. 2004; 101(21): 8168–8173, doi: 10.1073/pnas.0402765101, indexed in Pubmed: 15148385.
9. Deepmala B, Slattery J, Kumar N, et al. Clinical trials of N-acetylcysteine in psychiatry and neurology: a systematic review. Neurosci Biobehav Rev. 2015; 55: 294–321, doi: 10.1016/j.neubiorev.2015.04.015, indexed in Pubmed: 25957927.
10. Denic A, Johnson AJ, Bieber AJ, et al. The relevance of animal models in multiple sclerosis research. Pathophysiology. 2011; 18(1): 21–29, doi: 10.1016/j.pathophys.2010.04.004, indexed in Pubmed: 20537877.

11. Dickey DT, Muldoon LL, Doolittle ND, et al. Effect of N-acetylcysteine route of administration on chemoprotection against cisplatin-induced toxicity in rat models. Cancer Chemother Pharmacol. 2008; 62(2): 235–241, doi: 10.1007/s00280-007-0597-2, indexed in Pubmed: 17909806.
12. Dodd S, Dean O, Copolov DL, et al. N-acetylcysteine for antioxidant therapy: pharmacology and clinical utility. Expert Opin Biol Ther. 2008; 8(12): 1955–1962, doi: 10.1517/14728220802517901, indexed in Pubmed: 18990082.
13. Dumont D, Noben JP, Moreels M, et al. Characterization of mature rat oligodendrocytes: a proteomic approach. J Neurochem. 2007; 102(2): 562–576, doi: 10.1111/j.1471-4159.2007.04575.x, indexed in Pubmed: 17442050.
14. Elbini DI, Jallouli M, Annabi A, et al. A minireview on N-acetylcysteine: an old drug with new approaches. Life Sci. 2016; 151: 359–363, doi: 10.1016/j.lfs.2016.03.003.
15. Fan C, Long Y, Wang L, et al. N-Acetylcysteine rescues hippocampal oxidative stress-induced neuronal injury suppression of p38/JNK signaling in depressed rats. Front Cell Neurosci. 2020; 14: 554613, doi: 10.3389/fncel.2020.554613, indexed in Pubmed: 33262689.
16. Fernandes J, Gupta GL. N-acetylcysteine attenuates neuroinflammation associated depressive behavior induced by chronic unpredictable mild stress in rat. Behav Brain Res. 2019; 364: 356–365, doi: 10.1016/j.bbr.2019.02.025, indexed in Pubmed: 30772427.
17. Franco PG, Silvestroff L, Soto EF, et al. Thyroid hormones promote differentiation of oligodendrocyte progenitor cells and improve remyelination after cuprizone-induced demyelination. Exp Neurol. 2008; 212(2): 458–467, doi: 10.1016/j.expneurol.2008.04.039, indexed in Pubmed: 18572165.
18. Freeman L, Garcia-Lorenzo D, Bottin L, et al. The neuronal component of gray matter damage in multiple sclerosis: A [^{11}C]flumazenil positron emission tomography study. Ann Neurol. 2015; 78(4): 554–567, doi: 10.1002/ana.24468.
19. Gibson EM, Purger D, Mount CW, et al. Neuronal activity promotes oligodendrogenesis and adaptive myelination in the mammalian brain. Science. 2014; 344(6183): 1252304, doi: 10.1126/science.1252304, indexed in Pubmed: 24727982.
20. Goldschmidt T, Antel J, König FB, et al. Remyelination capacity of the MS brain decreases with disease chronicity. Neurology. 2009; 72(22): 1914–1921, doi: 10.1212/WNL.0b013e3181a8260a, indexed in Pubmed: 19487649.
21. Grothe M, Lotze M, Langner S, et al. The role of global and regional gray matter volume decrease in multiple sclerosis. J Neurol. 2016; 263(6): 1137–1145, doi: 10.1007/s00415-016-8114-3, indexed in Pubmed: 27094570.
22. Gudi V, Gingele S, Skripuletz T, et al. Glial response during cuprizone-induced de- and remyelination in the CNS: lessons learned. Front Cell Neurosci. 2014; 8: 73, doi: 10.3389/fncel.2014.00073, indexed in Pubmed: 24659953.
23. Hayat MA. Principles and Techniques of electron microscopy: Biological Applications. 4th ed. Cambridge University Press 2000: 37–59.
24. Hibbits N, Pannu R, Wu TJ, et al. Cuprizone demyelination of the corpus callosum in mice correlates with altered social interaction and impaired bilateral sensorimotor coordination. ASN Neuro. 2009; 1(3), doi: 10.1042/AN20090032, indexed in Pubmed: 19650767.
25. Hibbits N, Yoshino J, Le TQ, et al. Astrogliosis during acute and chronic cuprizone demyelination and implications for remyelination. ASN Neuro. 2012; 4(6): 393–408, doi: 10.1042/AN20120062, indexed in Pubmed: 23025787.
26. Kiernan JA. Dyes. In: Kiernan JA (eds). Histological and Histochemical Methods: Theory and Practice. 3rd ed. CRC Press 2000: 74–140.
27. Konopaske G, Dorph-Petersen KA, Sweet R, et al. Effect of chronic antipsychotic exposure on astrocyte and oligodendrocyte numbers in macaque monkeys. Biol Psychiatry. 2008; 63(8): 759–765, doi: 10.1016/j.biopsych.2007.08.018.
28. Kristensen TD, Mandl RCW, Jepsen JRM, et al. Non-pharmacological modulation of cerebral white matter organization: a systematic review of non-psychiatric and psychiatric studies. Neurosci Biobehav Rev. 2018; 88: 84–97, doi: 10.1016/j.neubiorev.2018.03.013, indexed in Pubmed: 29550210.
29. Llewellyn BD. Nuclear staining with alum hematoxylin. Biotech Histochem. 2009; 84(4): 159–177, doi: 10.1080/10520290903052899, indexed in Pubmed: 19579146.
30. Love S. Demyelinating diseases. J Clin Pathol. 2006; 59(11): 1151–1159, doi: 10.1136/jcp.2005.031195, indexed in Pubmed: 17071802.
31. Macarthur J, Papanikolaou T. The Cuprizone Mouse Model. 2014. http://www.msdiscovery.org/research-resources/animal-models/10993-cuprizone-mouse-model.
32. Manrique-Hoyos N, Jürgens T, Grønborg M, et al. Late motor decline after accomplished remyelination: Impact for progressive multiple sclerosis. Ann Neurol. 2012; 71(2): 227–244, doi: 10.1002/ana.22681.
33. Mierzwa AJ, Marion CM, Sullivan GM, et al. Components of myelin damage and repair in the progression of white matter pathology after mild traumatic brain injury. J Neuropathol Exp Neurol. 2015; 74(3): 218–232, doi: 10.1097/NEN.0000000000000165, indexed in Pubmed: 25668562.
34. Miller E, Wachowicz B, Majsterek I. Advances in antioxidative therapy of multiple sclerosis. Curr Med Chem. 2013; 20(37): 4720–4730, doi: 10.2174/09298673113209990156, indexed in Pubmed: 23834174.
35. Miller RH, Fyffe MS, Caprariello AC. Animal Models for the Study of Multiple Sclerosis In: Michael Conn P. (eds). Animal Models for the Study of Human Disease. 2nd ed. Academic Press 2017: 967–948.
36. Mohammed W, Radwan R, Elsayed H. Prophylactic and Ameliorative Effect of N-Acetylcysteine on Doxorubicin-Induced Neurotoxicity in Wister Rats. Egypt J Basic Clin Pharmacol. 2019; 9, doi: 10.32527/2019/101396.
37. Monti DA, Zabrecky G, Leist TP, et al. N-acetyl cysteine administration is associated with increased cerebral glucose metabolism in patients with multiple sclerosis: an exploratory study. Front Neurol. 2020; 11: 88, doi: 10.3389/fneur.2020.00088, indexed in Pubmed: 32117038.
38. Muniroh M. Methylmercury-induced pro-inflammatory cytokines activation and its preventive strategy using anti-inflammation N-acetyl-l-cysteine: a mini-review. Rev Environ Health. 2020; 35(3): 233–238, doi: 10.1515/reveh-2020-0026, indexed in Pubmed: 32710722.

39. Oakden W, Bock NA, Al-Ebraheem A, et al. Early regional cuprizone-induced demyelination in a rat model revealed with MRI. NMR Biomed. 2017; 30(9), doi: 10.1002/nbm.3743, indexed in Pubmed: 28544286.
40. Park D, Shin K, Choi EK, et al. Protective effects of N-acetyl-L-cysteine in human oligodendrocyte progenitor cells and restoration of motor function in neonatal rats with hypoxic-ischemic encephalopathy. Evid Based Complement Alternat Med. 2015; 2015: 764251, doi: 10.1155/2015/764251, indexed in Pubmed: 25918547.
41. Pohl HBF, Porcheri C, Mueggler T, et al. Genetically induced adult oligodendrocyte cell death is associated with poor myelin clearance, reduced remyelination, and axonal damage. J Neurosci. 2011; 31(3): 1069–1080, doi: 10.1523/JNEUROSCI.5035-10.2011, indexed in Pubmed: 21248132.
42. Saraswathy GR, Maheswari E, Santhrani T, et al. N-acetylcysteine alleviates phenytoin-induced behavioral abnormalities in rats. IJPSR. 2014; 5(8): 3279–92.
43. Skripuletz T, Gudi V, Hackstette D, et al. De- and remyelination in the CNS white and grey matter induced by cuprizone: the old, the new, and the unexpected. Histol Histopathol. 2011; 26(12): 1585–1597, doi: 10.14670/HH-26.1585, indexed in Pubmed: 21972097.
44. Skvarc DR, Dean OM, Byrne LK, et al. The effect of N-acetylcysteine (NAC) on human cognition: a systematic review. Neurosci Biobehav Rev. 2017; 78: 44–56, doi: 10.1016/j.neubiorev.2017.04.013, indexed in Pubmed: 28438466.
45. Snider DP. Adjuvant-free polyclonal antibody response manipulated by antibody-mediated antigen targeting In: Malik VS, Lillehoj EP, (eds). Antibody Techniques. 1st ed. Academic Press 1994: 49–70.
46. Song Q, Feng YB, Wang L, et al. COX-2 inhibition rescues depression-like behaviors via suppressing glial activation, oxidative stress and neuronal apoptosis in rats. Neuropharmacology. 2019; 160: 107779, doi: 10.1016/j.neuropharm.2019.107779, indexed in Pubmed: 31539536.
47. Stanislaus R, Gilg AG, Singh AK, et al. N-acetyl-L-cysteine ameliorates the inflammatory disease process in experimental autoimmune encephalomyelitis in Lewis rats. J Autoimmune Dis. 2005; 2(1): 4, doi: 10.1186/1740-2557-2-4, indexed in Pubmed: 15869713.
48. Steelman AJ, Thompson JP, Li J. Demyelination and remyelination in anatomically distinct regions of the corpus callosum following cuprizone intoxication. Neurosci Res. 2012; 72(1): 32–42, doi: 10.1016/j.neures.2011.10.002, indexed in Pubmed: 22015947.
49. Taraboletti A, Walker T, Avila R, et al. Cuprizone intoxication induces cell intrinsic alterations in oligodendrocyte metabolism independent of copper chelation. Biochemistry. 2017; 56(10): 1518–1528, doi: 10.1021/acs.biochem.6b01072, indexed in Pubmed: 28186720.
50. Tasset I, Agüera E, Sánchez-López F, et al. Peripheral oxidative stress in relapsing-remitting multiple sclerosis. Clin Biochem. 2012; 45(6): 440–444, doi: 10.1016/j.clinbiochem.2012.01.023, indexed in Pubmed: 22330938.
51. Tobin JE, Xie M, Le TQ, et al. Reduced axonopathy and enhanced remyelination after chronic demyelination in fibroblast growth factor 2 (Fgf2)-null mice: differential detection with diffusion tensor imaging. J Neuropathol Exp Neurol. 2011; 70(2): 157–165, doi: 10.1097/NEN.0b013e31820937e4, indexed in Pubmed: 21343885.
52. Van Munster CEP, Jonkman LE, Weinstein HC, et al. Gray matter damage in multiple sclerosis: Impact on clinical symptoms. Neuroscience. 2015; 303: 446–461, doi: 10.1016/j.neuroscience.2015.07.006, indexed in Pubmed: 26164500.
53. Vana AC, Flint NC, Harwood NE, et al. Platelet-derived growth factor promotes repair of chronically demyelinated white matter. J Neuropathol Exp Neurol. 2007; 66(11): 975–988, doi: 10.1097/NEN.0b013e3181587d46, indexed in Pubmed: 17984680.
54. Vargas DL, Tyor WR. Update on disease-modifying therapies for multiple sclerosis. J Investig Med. 2017; 65(5): 883–891, doi: 10.1136/jim-2016-000339, indexed in Pubmed: 28130412.
55. Vega-Riquer J, Mendez-Victoriano G, Morales-Luckie R, et al. Five decades of cuprizone, an updated model to replicate demyelinating diseases. Curr Neuropharmacol. 2019; 17(2): 129–141, doi: 10.2174/1570159x15666170717120343.
56. Voss EV, Škuljec J, Gudi V, et al. Characterisation of microglia during de- and remyelination: can they create a repair promoting environment? Neurobiol Dis. 2012; 45(1): 519–528, doi: 10.1016/j.nbd.2011.09.008, indexed in Pubmed: 21971527.
57. Wergeland S, Torkildsen Ø, Myhr KM, et al. The cuprizone model: regional heterogeneity of pathology. APMIS. 2012; 120(8): 648–657, doi: 10.1111/j.1600-0463.2012.02882.x, indexed in Pubmed: 22779688.
58. Wu JH, Batist G. Glutathione and glutathione analogues; therapeutic potentials. Biochim Biophys Acta. 2013; 1830(5): 3350–3353, doi: 10.1016/j.bbagen.2012.11.016, indexed in Pubmed: 23201199.
59. Zendedel A, Beyer C, Kipp M. Cuprizone-induced demyelination as a tool to study remyelination and axonal protection. J Mol Neurosci. 2013; 51(2): 567–572, doi: 10.1007/s12031-013-0026-4, indexed in Pubmed: 23666824.
60. Zhen W, Liu A, Lu J, et al. An alternative cuprizone-induced demyelination and remyelination mouse model. ASN Neuro. 2017; 9(4): 1759091417725174, doi: 10.1177/1759091417725174, indexed in Pubmed: 28840755.
61. Zhou J, Terluk MR, Basso L, et al. N-acetylcysteine provides cytoprotection in murine oligodendrocytes through heme oxygenase-1 activity. Biomedicines. 2020; 8(8), doi: 10.3390/biomedicines8080240, indexed in Pubmed: 32717964.